Title

Mitotic Spindle Positioning in the EMS Cell of Caenorhabditis elegans Requires LET-99 and LIN-5/NuMA

Journal

Genetics, 204(3)

ISSN

0016-6731

Authors

Liro, Małgorzata J
Rose, Lesilee S

Publication Date

2016-11-01

DOI

10.1534/genetics.116.192831

Peer reviewed

Mitotic Spindle Positioning in the EMS Cell of *Caenorhabditis elegans* Requires LET-99 and LIN-5/NuMA

Małgorzata J. Liro and Lesilee S. Rose[1]
Department of Molecular and Cellular Biology, University of California Davis, California 95616

ABSTRACT Asymmetric divisions produce daughter cells with different fates, and thus are critical for animal development. During asymmetric divisions, the mitotic spindle must be positioned on a polarized axis to ensure the differential segregation of cell fate determinants into the daughter cells. In many cell types, a cortically localized complex consisting of Gα, GPR-1/2, and LIN-5 (Gαi/Pins/Mud, Gαi/LGN/NuMA) mediates the recruitment of dynactin/dynein, which exerts pulling forces on astral microtubules to physically position the spindle. The conserved PAR polarity proteins are known to regulate both cytoplasmic asymmetry and spindle positioning in many cases. However, spindle positioning also occurs in response to cell signaling cues that appear to be PAR-independent. In the four-cell *Caenorhabditis elegans* embryo, Wnt and Mes-1/Src-1 signaling pathways act partially redundantly to align the spindle on the anterior/posterior axis of the endomesodermal (EMS) precursor cell. It is unclear how those extrinsic signals individually contribute to spindle positioning and whether either pathway acts via conserved spindle positioning regulators. Here, we genetically test the involvement of Gα, LIN-5, and their negative regulator LET-99, in transducing EMS spindle positioning polarity cues. We also examined whether the *C. elegans* ortholog of another spindle positioning regulator, DLG-1, is required. We show that LET-99 acts in the Mes-1/Src-1 pathway for spindle positioning. LIN-5 is also required for EMS spindle positioning, possibly through a Gα- and DLG-1-independent mechanism.

KEYWORDS asymmetric division; Src; Wnt; LET-99; NuMA

HIGHLY controlled mechanisms of spindle positioning underlie both symmetric and asymmetric cell divisions. In the case of asymmetric divisions, the position of the spindle specifies the plane of division and, thus, is critical for proper segregation of cell fate determinants into the differentially fated daughter cells. In addition, the plane of cell division affects daughter cell placement, which influences the morphogenesis of tissues and organs within an organism. Much of our understanding of spindle positioning has come from studies of asymmetric division in the one-cell *Caenorhabditis elegans* embryo and *Drosophila melanogaster* embryonic neuroblasts. Later research in vertebrate epithelial cells provided evidence for the conservation of the spindle positioning pathways. In all of these cell types, intrinsic PAR polarity proteins occupy distinct cortical domains to regulate cytoplasmic asymmetry and spindle positioning. A conserved complex of Gα/GPR/LIN-5 (Gα/Pins/Mud in *Drosophila* and Gα/LGN/NuMA in vertebrate cells) anchored at the cell cortex acts downstream of PAR proteins to recruit the microtubule motor protein dynein, which pulls on astral microtubules to physically position the nuclear-centrosome complex and spindle (Hao *et al.* 2010; Rodriguez-Fraticelli *et al.* 2010; Zheng *et al.* 2010; Morin and Bellaiche 2011; McNally 2013; Rose and Gonczy 2014; Williams *et al.* 2014).

LIN-5 (NuMA, Mud) was shown to be a direct link to dynein and GPR-1/2 (LGN, Pins) (Du and Macara 2004; Siller *et al.* 2006; Couwenbergs *et al.* 2007; Nguyen-Ngoc *et al.* 2007). NuMA and Mud have also been shown to be required for spindle positioning in association with additional components, and in some cases without Gα, or LGN/Pins. For example, in the *Drosophila* sensory organ precursor cell (SOP), the Wnt planar cell polarity pathway orients the spindle both with respect to the plane of the epithelium and on

doi: 10.1534/genetics.116.192831
Manuscript received June 17, 2016; accepted for publication September 16, 2016; published Early Online September 23, 2016.
Supplemental material is available online at www.genetics.org/lookup/suppl/doi:10.1534/genetics.116.192831/-/DC1.
[1]Corresponding author: Department of Molecular and Cellular Biology, One Shields Ave., University of California Davis, CA 95616. E-mail: lsrose@ucdavis.edu

the anterior/posterior (A/P) axis of the organism. The first orientation involves the Gα/Pins/Mud complex, but the latter involves direct recruitment of Mud by the Wnt component, Dishevelled, independent of Gα and Pins (Bellaiche *et al.* 2001a,b; David *et al.* 2005; Segalen *et al.* 2010). A similar planar cell polarity-directed pathway that requires Dsh, NuMA, and actin regulators aligns spindles during zebrafish gastrulation (Segalen *et al.* 2010; Castanon *et al.* 2013). In vertebrate cells that divide in parallel to the substrate, NuMA can also be recruited to the cortex independently of LGN at anaphase. This requires the ERM family proteins, phospholipids, and actin (Kiyomitsu and Cheeseman 2013; Seldin *et al.* 2013; Kotak *et al.* 2014; Zheng *et al.* 2014).

Despite considerable progress, much remains to be learned about mechanisms of spindle positioning, especially in response to multiple signaling pathways. The asymmetric division of the endomesodermal precursor (EMS) cell in the four-cell *C. elegans* embryo is an excellent model for understanding the coordination of multiple cues. In the EMS cell, the PAR domains exhibit an inner/outer polarity that is dependent on cell–cell contacts (Nance and Priess 2002). Thus, the PAR domains are not aligned with the spindle as they are in the well-characterized one-cell and P1 divisions. Rather, the EMS spindle aligns with the A/P axis in response to partially redundant Wnt and Mes-1 polarity cues that come from the neighboring posterior cell, called P2 (Figure 1A and Figure 2A). In the absence of both cues, the EMS blastomere divides on the left/right (L/R) axis and fails to specify endoderm (Bei *et al.* 2002).

Genetic experiments showed that the upstream components of the Wnt signaling pathway, such as the Wnt ligand (MOM-2 in *C. elegans*), the Frizzled receptor (MOM-5), and the Disheveled adaptor proteins (DSH-2 and MIG-5), play a role in EMS spindle positioning (Figure 2A); however, this activity is independent of the transcriptional activation associated with canonical Wnt signaling (Schlesinger *et al.* 1999; Bei *et al.* 2002). The Mes-1 pathway acts in parallel to the Wnt pathway (Figure 2A) and has only two confirmed components based on localization and genetic studies. First, MES-1, a receptor tyrosine kinase-like protein, localizes to the P2/EMS cell contact (Berkowitz and Strome 2000; Bei *et al.* 2002). Second, the cortical enrichment of the activated form of SRC-1 kinase at the P2/EMS contact site is mediated by MES-1 (Liu *et al.* 2010). Both *mes-1* and *src-1* single mutants have been shown to enhance the EMS spindle positioning defects seen in Wnt pathway single mutants, but they do not enhance each other (Bei *et al.* 2002).

A potential downstream effector of spindle positioning in both the Wnt and Mes-1/Src-1 pathways is dynactin, an activator of dynein. Downregulation of dynactin by RNA interference (RNAi) results in spindle positioning defects in EMS, and dynactin enrichment at the P2/EMS contact in wild-type embryos was shown to depend on both Wnt and SRC-1 (Zhang *et al.* 2008). Because Wnt is required for EMS but not P2 spindle positioning (Schlesinger *et al.* 1999; Bei *et al.* 2002), the Wnt pathway is proposed to recruit dynein and mediate cortical force generation specifically in the EMS blastomere. However, SRC-1 is also required for EMS and P2 spindle positioning (Bei *et al.* 2002), so it is not clear whether the effect on dynactin enrichment is occurring in the EMS, the P2 blastomere, or in both cells. LIN-5 is also enriched at the P2/EMS contact (Srinivasan *et al.* 2003; Fisk Green *et al.* 2004), and is known to mediate dynein recruitment to the cortex at the one- and two-cell stage (Nguyen-Ngoc *et al.* 2007). However, the role of LIN-5 in EMS spindle positioning has never been tested.

Two other proteins that may participate in EMS spindle positioning are LET-99 and Gα. LET-99, a DEP domain-containing protein (Dishevelled, Egl-10 and Pleckstrin domain), has a well-established role in mediating spindle positioning during the first asymmetric division, downstream of the PAR proteins. LET-99 antagonizes Gα activity, and in the one-cell zygote (P0), LET-99 inhibits the localization of GPR-1/2 and LIN-5 from the lateral-posterior cortical domain, thus generating asymmetry of cortical pulling forces (Rose and Kemphues 1998; Tsou *et al.* 2002, 2003a; Wu and Rose 2007; Park and Rose 2008; Krueger *et al.* 2010). P0 divides asymmetrically to produce a larger AB daughter cell and a smaller, posterior P1 daughter cell. The AB cell divides symmetrically giving rise to ABa and ABp; P1 undergoes another round of asymmetric cell division on the A/P axis to produce EMS and P2 (Figure 1A). The PAR proteins, LET-99, GPR-1/2, and LIN-5, are asymmetrically localized at the P1 cortex and they are required for spindle positioning, as in the one-cell, P0 (Rose and Gonczy 2014). In contrast, there is no band pattern of LET-99 in the EMS cell; instead, cortical LET-99 appears lower at the P2/EMS cell contact site, whereas GPR-1/2 and LIN-5 are more enriched (Srinivasan *et al.* 2003; Tsou *et al.* 2003a). We and others previously showed that the inactivation of LET-99 and Gα at the two-cell stage using temperature-sensitive (ts) alleles resulted in failure of EMS spindle rotation, suggesting a potential role for these proteins in EMS spindle positioning (Tsou *et al.* 2003a; Zhang *et al.* 2008). However, in both *let-99(ts)* and *Gα* mutant embryos there are gross perturbations of the ABa and ABp spindle orientations, which can distort the shape of the EMS cell. Further, our reexamination of the *let-99(ts)* mutant using a temperature-controlled microscope stage revealed defects in the P1 division, even at the supposed permissive temperature (see *Materials and Methods*), raising the possibility that the EMS division defects reported were indirect.

In this report, we examine the requirement of LET-99, Gα, and LIN-5 in EMS spindle positioning, and test whether these proteins are part of the Wnt or Mes-1/Src-1 pathways. Single-mutant analysis using additional *let-99* temperature-sensitive alleles that can be specifically inactivated at the four-cell stage, together with an examination of *lin-5(ts)* and *gpa-16(ts)* mutants, revealed EMS spindle positioning defects only in *lin-5(ts)* embryos. However, double-mutant analysis indicates that LET-99 functions in the Mes-1/Src-1 pathway for EMS spindle positioning.

Materials and Methods

Worm strains

C. elegans were grown using standard conditions (Brenner 1974). Published strains used were as follows: AZ244 *unc-119(ed3) III*; *ruIs57[pie-1*::*GFP*::*tubulin* + *unc-119(+)]* (Praitis *et al.* 2001); BW1808 *gpa-16(it143) unc-13(e51) I* (Bergmann *et al.* 2003); EU452, *mom-5(zu193) unc-13(e1091)/hT2 I*; *+/hT2[bli-4(e937)let(h661)] III* (Schlesinger *et al.* 1999); EU1100 *let-99*(or513) *IV* (Goulding *et al.* 2007); FM102 *lin-5(ev571)ts*; *GFP*::*tubulin* (Park and Rose 2008); SS149 *mes-1(bn7) X* (Capowski *et al.* 1991; Strome *et al.* 1995); RL264 *let-99* (ax218)*unc-30 (e191) IV* (Wu *et al.* 2016); and EU660 *let-99(or204) IV* (Encalada *et al.* 2000; Goulding *et al.* 2007). BW1808, EU452, RL264, and SS149 were crossed to AZ244 to create RL262, RL302, RL292, and RL265, respectively for this study: RL262 *mom-5(zu193) unc-13(e1091)/hT2 I*; *+/hT2[bli-4(e937)let(h661)]*; *unc-119(ed3) III*; *ruIs57[pie-1*::*GFP*::*tubulin* + *unc-119(+)]*; RL302 *gpa-16(it143) unc-13(e51) I*; *unc-119(ed3) III*; *ruIs57[pie-1*::*GFP*::*tubulin* + *unc-119(+)]*; RL292 *mes-1(bn7) X*; *unc-119(ed3) III*; *ruIs57[pie-1*::*GFP*::*tubulin* + *unc-119(+)]*; and RL265 *let-99* (ax218)*unc-30 (e1919) IV*; *unc-119(ed3) III*; *ruIs57 [pie-1*::*GFP*::*tubulin* + *unc-119(+)]*. *EU660* was outcrossed to N2 four times to generate RL220 *let-99(or204)*. Strains were grown at 15–16° unless otherwise indicated.

RNA interference

RNAi was carried out by bacterial feeding (Timmons and Fire 1998) using the following Ahringer library clones (Kamath *et al.* 2003): *mes-1*(X-5L23), *mom-2*(V-6A13), *mig-5*(II-6C13), *dsh-2*(II-4011), *dlg-1*(X-8A08), *goa-1*(I-3P15), and *gpa-16* from Park and Rose (2008). Bacteria were used undiluted for single RNAi, or mixed 1:1 for double RNAi. Feeding was conducted at 15–16° for 36–48 hr unless otherwise stated for specific experiments. *dlg-1* RNAi was achieved by feeding for at least 24 hr at room temperature (23–25°) and then embryos were imaged at 25°. Effectiveness of the *dlg-1(RNAi)* was confirmed by high embryo lethality (93% lethality after 24 hr of RNAi feeding and 100% lethality following 48 hr of feeding). *src(RNAi)* (Cram *et al.* 2006) feeding resulted in 66% lethality after 24 hr and in 97% lethality following 48 hr of feeding at room temperature.

Imaging and temperature shifts

Embryos were removed from gravid hermaphrodites and mounted on 2% agarose pads under coverslips. Single-plane images were acquired every 10 sec on an Olympus BX60 microscope equipped with PlanApo N 60X, 1.42 NA objective lens, a Hammatasu Orca 12-bit digital camera, and OpenLab Software. Worms were imaged with a combination of epifluorescence and brightfield; the latter minimized photodamage in addition to allowing better assessment of final daughter cell positions. As such, data in Figure 2B comes from a subset of embryos where early centrosome migration patterns were scorable by epifluorescence. For spindle positioning data sets, embryos were scored as follows unless noted in the figure legend: division was "A/P" if both centrosomes were visible on the A/P axis prior to nuclear envelope breakdown (NEB) as in the wild type, and the final daughter positions were on the A/P axis. Often, one centrosome/spindle pole was slightly out of focus because the EMS spindle is at a slight angle to the L/R midline even in control embryos (*e.g.*, see Figure 1C; the L/R axis is into the plane of the image in most embryos filmed on agar). Based on analysis of the *z*-plane, we estimate that any spindle with both centrosomes visible is within 45° of the midline along the A/P axis. In embryos scored as exhibiting a late rotation, the centrosomes were not visible on the A/P axis prior to NEB, but the spindle moved to within the normal A/P range before cytokinesis onset. Spindles that did not rotate and divided at an angle between 45 and 90° to the A/P axis [which could be L/R, D/V (dorsal/ventral), or oblique] were placed in the L/R / D/V category. In general, the spindle formed on the axis defined by the final position of the centrosomes after migration, but sometimes the spindle shifted in the L/R or D/V axis as the ABa/p division proceeded and the embryo changed shape. Chi-squared statistical analysis of spindle positioning was done in Excel. Graphs were made in GraphPad Prism Version 6.0.

Temperature shifts were performed by placing the slide on a Linkam PE95/T95 System Controller with an Eheim Water Circulation Pump. The true temperature of the slide was determined by inserting the wire probe of an Omega HH81 digital thermometer between the cover slip and an agar pad with the 60 × objective and oil in place. The permissive temperature for all experiments was 16.4–17.4° (controller temperature set to 8°) and the nonpermissive temperature was 25.0–25.1° for most experiments, or 26° for some *lin-5(ts)* experiments (controller set to 25° and 26°, respectively). To prevent inactivation during slide preparation, ice packs were placed around the dissecting microscope, and slides with agar pads, coverslips, and buffer were kept on ice to maintain temperature below 16°.

To determine how quickly temperature-sensitive alleles became inactivated, *lin-5(ev571ts)* and *let-99(ax218ts)* strains were grown at 15–16° and then upshifted prior to the P1 division. *lin-5(ev571ts)*, *let-99(ax218ts)*, and *let-99(or513ts)* required 4–5 min at the nonpermissive temperature to cause a complete failure of P1 spindle rotation. For the analysis of EMS spindle positioning, *lin-5(ev571ts)* embryos were upshifted during or before the ABa/p centrosome separation but no later than NEB of ABa/p. *let-99*(ax218)*ts* embryos were upshifted after the ABa/p centrosome separation to avoid spindle positioning defects in those cells. In both cases, the temperature upshifts were complete more than 5 min before the predicted EMS nuclear centrosome rotation, as determined from *GFP*::*tubulin* embryos imaged at 25°. A total of 10% of *lin-5(ev571ts)* embryos exhibited failure of P1 nuclear rotation even at the permissive temperature, as did 12% of *let-99(ax218ts)* and 32% of *let-99(or513ts)*. Only embryos that exhibited normal or late rotation and, thus, still divided asymmetrically were analyzed for EMS spindle positioning.

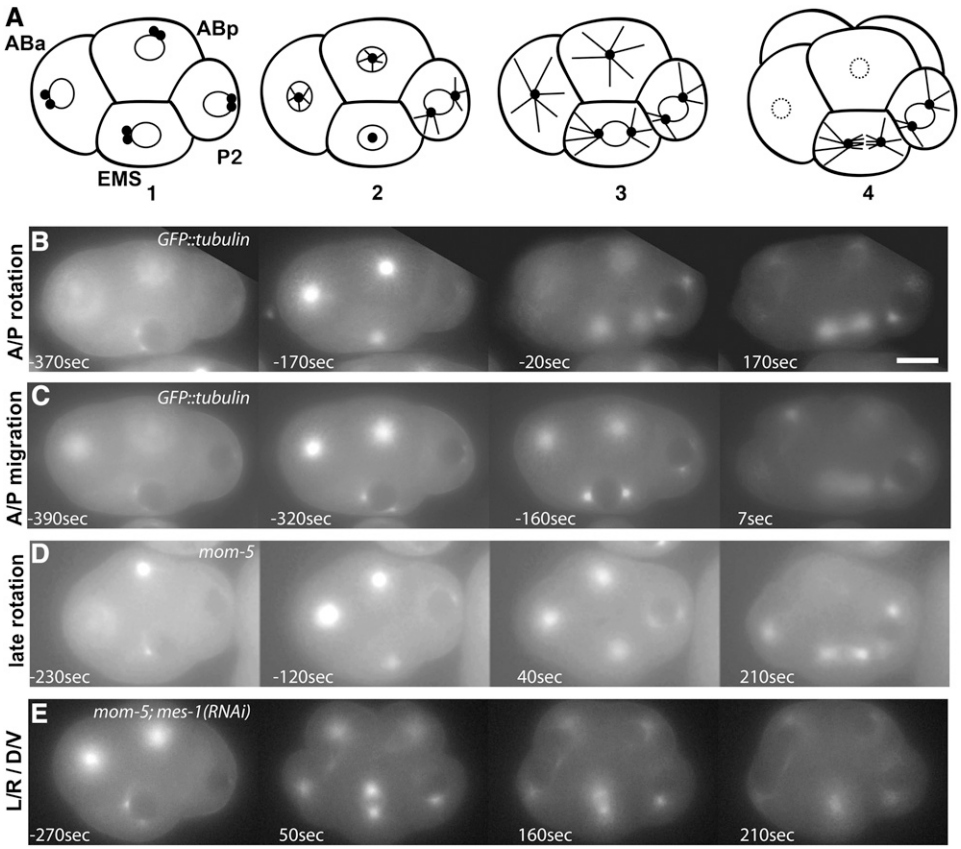

Figure 1 EMS spindle positioning visualized in GFP::tubulin-expressing embryos. (A) Schematic of centrosome migration and spindle positioning exhibited by the majority of control embryos at the four-cell stage. The EMS centrosomes migrate from an anterior position (1) onto the L/R axis (2), and then the nuclear centrosome complex rotates onto the A/P axis (3) where the spindle forms following NEB (4). (B–E) Epiflourescence images of *GFP::tubulin*-expressing control embryos, *mom-5* mutant embryos, and *mom-5; mes-1(RNAi)* embryos. Time points relative to NEB are indicated (negative numbers, time before NEB; positive numbers, time after NEB). (B) An example of centrosomes separating onto the L/R axis followed by nuclear-centrosome rotation onto the A/P axis. (C) An embryo in which centrosomes migrate directly on to the A/P axis. (D) An example of an embryo in which the centrosomes migrated onto the L/R axis and spindle rotation onto the A/P axis occurred late, after NEB. (E) An embryo in which neither nuclear or late spindle rotation occurred, and the final spindle was oriented between the L/R and D/V axes. A/P, anterior/posterior; D/V, dorso/ventral; EMS, endomesodermal precursor; L/R, left/right; NEB, nuclear envelope breakdown; RNAi, RNA interference.

Embryos from the *gpa-16(it143ts)* single-mutant strain were upshifted at various times during the one- to four-cell stage to determine a minimal upshift time. However, there was no correlation between the duration of temperature upshift and the P1 phenotype: early one-cell embryos often had normal P1 rotation, while embryos upshifted later at the early two-cell stage sometimes exhibited abnormal P1 rotations. Overall, 33% of upshifted embryos exhibited failure of P1 rotation (Supplemental Material, Figure S2A), compared to 75% P1 rotation defects ($N = 12$) observed when worms were grown at 25° overnight, similar to previous reports (Bergmann *et al.* 2003). This indicates that *it143* is not a fast-inactivating ts allele, but nonetheless upshift at the one- to two-cell stage causes a loss-of-function.

For the *gpa-16(ts);goa-1(RNAi)* data shown in Figure S2, B and C, *gpa-16(ts)* worms were grown on *goa-1* RNAi for 36–48 hr at 15–16° and then imaged at 25° using the temperature-controlled stage. To try to obtain embryos in which the AB, P1, and ABa/p divisions were normal, *gpa-16(ts)* worms were also grown at a lower permissive temperature of 14–15° for 22–27 hrs of *goa-1* RNAi treatment. Nonetheless, 5/7 embryos had an abnormal AB and/or P1 division, and 7/7 ABa/p divisions were misoriented, resulting in embryos with highly abnormal cell arrangements. Thus, we were not able to observe EMS spindle positioning defects in the absence of other division abnormalities.

Immunofluorescence

Immunolocalization was carried out on *gpa-16(it143ts);goa-1(RNAi)* and *goa-1(sa734)*; *gpa-16(RNAi)* embryos that were upshifted to 25° for 24–50 hr. Immunolocalization was performed using a standard liquid nitrogen freeze-fracture method followed by −20° methanol fixation as described previously (Park and Rose 2008). Rat anti-LIN-5 antibodies were diluted 1:50 in PBS-Tween (PBST), and rhodamine goat anti-rat secondary antibodies were diluted 1:100 in PBST. DAPI staining was used to visualize DNA. Secondary antibodies were preabsorbed with acetone powder from wild-type worms. Specimens were mounted with Vectashield (Vector Laboratories) and imaged using a 60X PLAPON NA 1.42 objective on an Olympus FV1000 Fluorview Laser Scanning Confocal Microscope. Ten 0.2-μm sections in the z-plane were taken at the midfocal plane of embryos using identical settings below saturation. Images shown in panels are maximum intensity z-projections made in Fiji. Fluorescence intensities of maximum intensity projections were traced using the segmented line tool of the Fiji software. Each cell–cell contact was measured at the four-cell stage; an adjacent cytoplasmic region from both cells was averaged. The ratios of the cortical to the cytoplasmic pixel intensities were then calculated for each cell–cell contact in the embryos, and were averaged for each genotype.

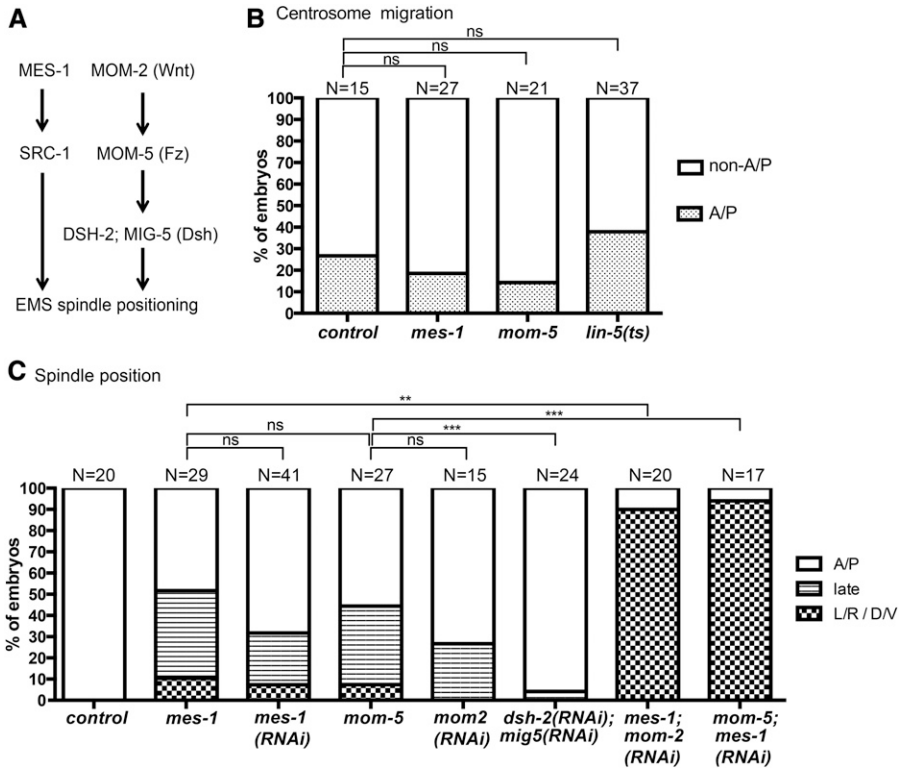

Figure 2 Wnt and Mes-1/Src-1 pathway mutants exhibit similar spindle positioning defects. (A) Summary of selected previously published components of the Wnt and Mes-1/Src-1 pathways required for EMS spindle positioning. Vertebrate orthologs are written in parentheses. (B) Quantification of centrosome migration directly on to the A/P axis *vs.* non-A/P axis positions. (C) Quantification of EMS spindle positioning. The A/P category includes embryos whose centrosomes migrated directly on to the A/P axis and ones whose nuclear-centrosome complex rotated onto the A/P axis before NEB. The late rotation category refers to EMS spindle alignment with the A/P axis that occurs after NEB; the L/R / D/V category includes final spindle positions on all non-A/P axes, as described in the *Materials and Methods*. Data were compared using Chi-squared analysis (ns, not significant, $P > 0.05$, * $P \leq 0.05$, ** $P \leq 0.01$, *** $P \leq 0.001$; see Table S1 for specific P values). A/P, anterior/posterior; D/V, dorso/ventral; EMS, endomesodermal precursor; L/R, left/right; NEB, nuclear envelope breakdown; RNAi, RNA interference.

Four-cell embryos quantified included early prophase through metaphase, based on DAPI staining and centrosome position as labeled by LIN-5. Statistical tests of significance were made using the Student's *t*-test in Excel and Prism. To assess RNAi effectiveness before fixation, the P1 and ABa/p cleavages were analyzed and only those treatments producing a strong Gα mutant phenotype were used. In addition, one-cell *gpa-16(it143ts);goa-1(RNAi)* mutant embryos were stained in parallel; LIN-5 cortical staining was barely detectable in most one-cell embryos (mean cortical to cytoplasmic ratio of 0.89, $n = 10$), as previously reported (Park and Rose 2008).

Data availability

Strains and antibodies are available upon request.

Results

Wnt and Mes-1/Src-1 pathway mutants have similar defects in nuclear rotation

Previous studies indicated that the centrosomes migrate onto the L/R axis in the EMS cell just as in the ABa/p cells (Figure 1, A and B) (Rose and Gonczy 2014). While the ABa/p spindles set up on the L/R axis defined by this centrosome positioning, in the EMS cell, the nuclear-centrosome complex rotates approximately 90° onto the A/P axis prior to nuclear envelope breakdown (NEB) (Figure 1A). Thus the EMS spindle forms on the A/P axis (Figure 1, A and B). Wnt mutants have been reported to fail in nuclear rotation but eventually orient onto the A/P axis in anaphase when EMS is analyzed in the intact embryo (Schlesinger *et al.* 1999). Mes-1/Src-1 pathway mutants have also been reported to exhibit late spindle rotations, but also to exhibit final spindle orientations on the L/R or the D/V axes (Bei *et al.* 2002; Kim *et al.* 2013). These observations raised the possibility that the Mes-1/Src-1 pathway could have a greater, or different, contribution to spindle positioning than the Wnt pathway. Therefore, we first carefully compared early centrosome movements and EMS spindle positioning between wild-type and single mutants of the Wnt and Mes-1/Src-1 pathway components using a combination of bright field and fluorescence time-lapse microscopy. To facilitate this analysis, mutations in the Frizzled ortholog of the Wnt pathway, *mom-5(zu193)*, and the *mes-1(bn7)* mutation were combined with a *GFP*::*tubulin* transgene.

In *GFP*::*tubulin*-expressing embryos, centrosome positions were more variable than described previously (Figure 1A and Figure 2B). We observed centrosome migration onto the D/V axis in addition to the L/R axis, or onto an axis in between those (referred to as oblique). Moreover, in 26.7% of control embryos, the centrosomes migrated directly onto the A/P axis (Figure 2B); thus, little to no rotation was needed for the spindle to form on the A/P axis (Figure 1C). Of the control *GFP*::*tubulin* embryos where the centrosomes migrated onto a non-A/P axis, all exhibited nuclear-centrosome rotation onto the A/P axis prior to NEB (Figure 1, A and B), as previously reported (Hyman and White 1987; Schlesinger *et al.* 1999; Bei *et al.* 2002). Therefore, the EMS spindle always formed on the A/P axis in *GFP*::*tubulin* control embryos, but the centrosomes arrived on that axis by more than one route.

Based on the analysis described above, it was possible that Wnt and Mes-1 signaling differentially affect early centrosome migration patterns in addition to nuclear-centrosome complex rotation. Therefore, we analyzed centrosome movements in embryos from either *mom-5* or *mes-1* mutant mothers (hereafter referred to as *mom-5* and *mes-1* embryos). Similar to the wild type, in both *mom-5* and *mes-1* mutant embryos, we observed migration of the centrosomes on to the L/R, D/V, or oblique axes (Figure 2B, "centrosome non-A/P migration"). Further, a proportion of *mes-1* and *mom-5* single-mutant embryos exhibited a direct migration onto the A/P axis (18.5 and 14.3%, respectively) (Figure 1C and Figure 2B), and there was no significant difference between *mom-5* and *mes-1* mutants or either mutant compared to wild-type (Figure 2B and Table S1). Similarly, in the subset of *mom-5; mes-1(RNAi)* double-mutant embryos in which the centrosome migration paths could be followed throughout the early cell cycle, 28.5% migrated onto the A/P axis directly ($n = 7$; Table S1). We conclude that early centrosome migration movements are not regulated by either the Wnt or Mes-1 pathways.

We also carefully examined nuclear rotation in *mom-5* and *mes-1* single-mutant embryos. In almost half of the embryos of both genotypes, nuclear rotation did not occur prior to NEB and thus the spindle formed on the D/V, L/R, or oblique axis. In most single-mutant embryos, the spindle then rotated onto the A/P axis following NEB; we classified such events as abnormal late rotations (Figure 1D). In a small proportion of both *mes-1* and *mom-5* embryos, the spindle never aligned with the A/P axis resulting in spindles positioned at D/V, L/R, or oblique non-AP angles (see *Materials and Methods*); we refer to these as D/V / L/R divisions (Figure 1E). The combined proportion of these two classes of abnormal EMS spindle positioning events was not statistically different between *mom-5* and *mes-1* single mutants, but both single mutants were different from controls (Figure 2C, Table S1).

RNAi greatly facilitates the generation of embryos depleted for components of both pathways. Therefore, we also compared spindle positioning after RNAi of *mes-1*, the Wnt ortholog, *mom-2*, and the partially redundant disheveled orthologs, *dsh-2* and *mig-5*. Similar EMS spindle positioning defects were observed between single mutants and RNAi-treated embryos (Figure 2C and Table S1). Further, the majority of *mes-1;mom-2(RNAi)* and *mom-5;mes-1(RNAi)* embryos showed a complete failure to correctly orient their spindle (Figure 1E and Figure 2C), as previously reported (Schlesinger *et al.* 1999; Bei *et al.* 2002). Late rotations were not observed in the double-mutant; the presence of a small number of A/P divisions in this and other double-mutant combinations is likely due to centrosomes migrating directly onto to the A/P axis, as noted for *mom-5;mes-1(RNAi)* embryos above. The defects observed with *dsh-2(RNAi);mig-5(RNAi)* embryos were weaker than in *mom-2(RNAi)* or *mom-5* embryos; nonetheless, *dsh-2;mig-5(RNAi)* in combination with *mes-1* yielded a strong double-mutant phenotype (Figure 2C and Table S1) and thus was also used for further studies. All together, these results suggest that the Wnt and Mes-1/Src-1 pathways contribute in similar ways to EMS nuclear rotation prior to NEB.

LIN-5 is required for EMS spindle positioning

To determine whether LIN-5 is involved in EMS spindle positioning, we imaged *lin-5(ev571ts)* embryos (Lorson *et al.* 2000) expressing *GFP*::*tubulin*. Because LIN-5 is required for posterior spindle displacement in the one-cell embryo and for nuclear rotation in the P1 cell of two-cell embryos, we utilized a temperature-controlled microscope stage for these studies (see *Materials and Methods*). We found that *lin-5(ts)* embryos shifted from permissive (16.4–17.4°) to nonpermissive (25–26°) temperature 5 min before P1 division exhibited a 100% failure of P1 nuclear rotation, indicating that this allele causes a strong loss of the LIN-5 protein function at the nonpermissive temperature. We next analyzed the requirement for LIN-5 in EMS spindle orientation by imaging *lin-5(ts)* embryos at permissive temperature and then upshifting during the early four-cell stage, at least 5 min before the normal time of EMS nuclear rotation. Under these conditions, a small subset of *lin-5(ts)* embryos exhibited a failure of P1 rotation at the permissive temperature, before the temperature upshift; therefore, only embryos in which the P1 oriented normally before division were analyzed further.

lin-5(ts) embryos upshifted at the early four-cell stage exhibited poor centrosome separation in all blastomeres as compared to wild-type. The forming EMS spindle appeared smaller and often bent at the time of NEB, but then became bipolar and spindle poles separated at anaphase (Figure 3, A and B). Nonetheless, we were able to score the position of most of the EMS centrosomes relative to the timing of NEB and the A/P axis. In 38% of *lin-5(ts)* embryos, the centrosomes migrated directly onto the A/P axis and thus the spindle formed on the correct axis (Figure 2B); this percentage is not statistically different from wild-type. Of the remaining *lin-5(ts)* embryos, many exhibited late nuclear rotation or L/R and D/V spindle orientations (Figure 3, B and C), similar to what was observed for *mes-1* and *mom-5* single mutants.

To determine if LIN-5 functions in either the Wnt or Mes-1/Src-1 pathway, we tested whether downregulation of signaling components could enhance the partial defects seen in *lin-5(ts)* embryos, as happens in double mutants of known components of these pathways. *lin-5(ts)* embryos treated with *mom-2* or *dsh-2;mig-5* RNAi did not show a statistically significant increase in the total abnormal EMS spindle positioning events compared to *lin-5(ts)* single mutants. Similarly, EMS spindle defects of *lin-5(ts)* embryos were not enhanced by *mes-1(RNAi)* (Figure 3C). These data suggest that LIN-5 is required for EMS spindle positioning but it is unclear whether LIN-5 is in the Wnt or Mes-1/Src-1 pathway.

LET-99 acts in the Mes-1/Src-1 pathway for EMS spindle positioning

Previously, it was shown that upshift of the *let-99(or204ts)* temperature-sensitive allele at the end of the P1 division

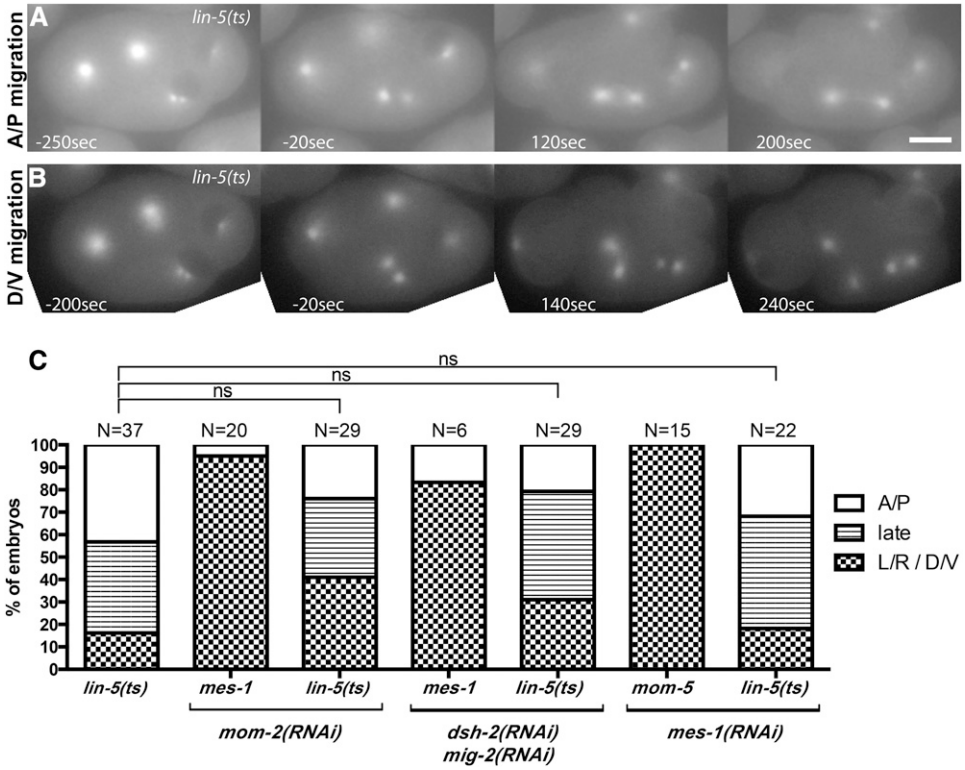

Figure 3 LIN-5 is required for EMS spindle positioning. (A–B) Epifluorescence images from time-lapse video microscopy of *GFP::tubulin*; *lin-5(ts)* embryos. (A) An embryo in which centrosomes migrated directly onto the A/P axis. (B) An example where centrosomes migrated on to the D/V axis, there was no nuclear rotation, and the final spindle position was D/V. (C) Quantification of EMS spindle positioning as in Figure 2C. The effectiveness of *mes-1(RNAi)* and *mom-2(RNAi)* treatments was confirmed by analyzing double-mutant/RNAi combinations of Wnt and Mes-1/Src-1 pathway components in parallel to *lin-5(ts); wnt(RNAi)/mes-1(RNAi)*. Over 80% of EMS divisions were abnormal in *mom2 (RNAi);mes-1*, *dsh-2:mig-2(RNAi);mes-1* and *mes-1(RNAi);mom-5* embryos. Data were compared using Chi-squared analysis (ns, not significant, $P > 0.05$; see Table S1 for specific *P* values). A/P, anterior/posterior; D/V, dorso/ventral; EMS, endomesodermal precursor; L/R, left/right; RNAi, RNA interference.

resulted in failure of EMS spindle rotation (Tsou *et al.* 2003a). However, these embryos were not imaged at permissive temperature during the P1 division; these embryos also exhibited abnormal AB cell divisions, raising the possibility that earlier defects affected the EMS division. Therefore, we used a temperature-controlled stage to image *let-99(ts)* conditional mutants at the permissive temperature, 16.4–17.4°, during the first two divisions, followed by temperature upshift to the restrictive temperature (25°) at the four-cell stage. Examination of the *let-99(or204ts)* embryos revealed that 60% ($N = 10$) of these embryos had failures of P1 nuclear rotation even at the permissive temperature, which could interfere with normal EMS and P2 specification. By contrast, the *let-99(ax218ts)* and *let-99*(or513)*ts* mutants exhibited fewer P1 rotation defects (12%, $N = 52$ and 32%, $N = 25$, respectively) at the permissive temperature and were therefore analyzed further. Temperature upshifts were carried out at least 5 min before the time of EMS nuclear rotation, allowing sufficient time for LET-99(ts) protein inactivation (see *Materials and Methods*). Embryos upshifted with this regimen exhibited normal ABa/p divisions, and only embryos in which P1 divided asymmetrically on the A/P axis were scored for the EMS division. The EMS centrosome migration patterns were similar to those described for wild-type, with direct A/P migration observed in 36.4% of *let-99*(ax218); *GFP::tubulin* embryos ($N = 11$, Table S1). Defects in EMS spindle positioning were only observed in 10% of *let-99(ts)* embryos using either allele; in these embryos, the spindle formed on the L/R axis but eventually rotated onto the A/P axis before cytokinesis (Figure 4A and Figure S1A).

We next examined *let-99(ts)* mutants that were also depleted for either Wnt or Mes-1/Src-1 pathway components and upshifted at the four-cell stage. In *let-99(ts)* embryos depleted for Wnt components, there was no enhancement of the EMS spindle positioning defects (Figure 4A and Figure S1A). Interestingly, the number of abnormal EMS spindle positioning events seen in *let-99(ts);mes-1(RNAi)* embryos appeared reduced compared to *mes-1(RNAi)* embryos, but the difference was not statistically significant. To test this potential interaction further, we treated *let-99(ts)* embryos with *src-1(RNAi)*. RNAi of *src-1* alone gave a stronger spindle positioning defect than *mes-1(RNAi)*, but < 20% of *src-1(RNAi);let-99(ts)* embryos exhibited such defects (Figure 4A, Figure S1A, and Table S1). We confirmed these suppression results by generating a *let-99(ax218ts);mes-1(bn7)* double-mutant. At the nonpermissive temperature, 15% of *let-99(ax218ts)*; *mes-1(bn7)* embryos exhibited EMS spindle positioning defects as compared to 55% *mes-1(bn7)* abnormal EMS divisions (Figure 4B). To test if loss of *let-99* could also suppress the *wnt;mes-1* double-mutant phenotype, we examined spindle positioning in *let-99(ax218ts);mes-1(bn7);mom-2(RNAi)* embryos. Although *let-99(ax218ts);mes-1(bn7); mom-2(RNAi)* embryos analyzed at the permissive temperature throughout the EMS division phenocopied the strong *wnt*; *mes-1* double-mutant phenotype, this phenotype was suppressed in embryos upshifted at the four-cell stage (Figure 4B). Together, these data suggest that LET-99 acts downstream of the Mes-1/Src-1 pathway, in parallel to the Wnt pathway.

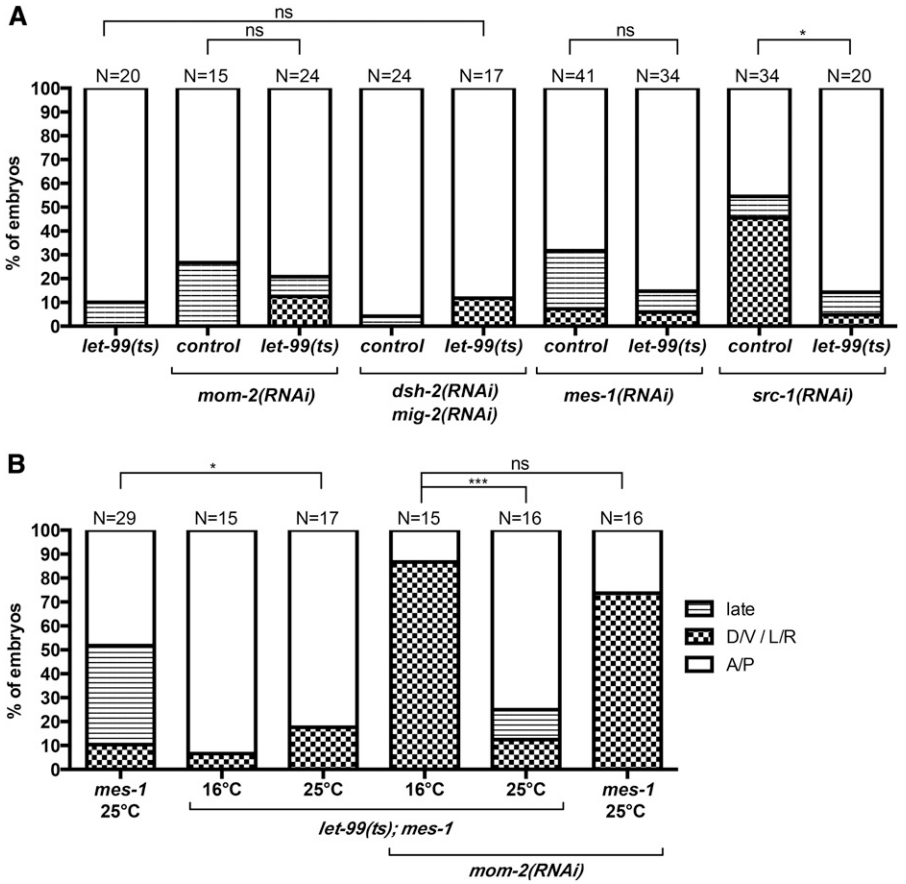

Figure 4 *let-99ts* suppresses *mes-1* and *src-1* spindle positioning defects. (A) Quantification of EMS spindle positioning in *let-99(ax218ts)* alone and in combination with depletion of Wnt and Mes-1/Src-1 pathway components. The effectiveness of *mes-1(RNAi)* and *mom-2-(RNAi)* treatments was confirmed by analyzing double-mutant combinations in parallel: 86% of *mes-1*; *mom-2(RNAi)* (N = 14), 100% of *mes-1*; *dsh-2:mig-2(RNAi)* (N = 16), and 94% of *mom-5*; *mes-1(RNAi)* (N = 17) embryos exhibited EMS spindle positioning defects. (B) Quantification of spindle positioning in *let-99(ax218ts);mes-1(bn7)* double mutants with and without depletion of the Wnt pathway component *mom-2*. The *let-99(ts)* combinations were grown and imaged constantly at permissive temperature (16°) or were shifted from the permissive to the nonpermissive temperature at the four-cell stage (25°). *mes-1* and *mes-1;mom-2(RNAi)* controls imaged at 25° are shown. Data were compared using Chi-squared analysis (ns, not significant, $P > 0.05$, * $P \leq 0.05$, ** $P \leq 0.01$, *** $P \leq 0.001$, see Table S1 for specific P values). A/P, anterior/posterior; D/V, dorso/ventral; EMS, endomesodermal precursor; L/R, left/right; RNAi, RNA interference.

The loss of one Gα, GPA-16, does not cause EMS spindle positioning defects

In *C. elegans*, GPA-16 and GOA-1 are two partially redundant *G*α proteins that form the Gα/GPR/LIN-5 complex and are required for early spindle positioning (Rose and Gonczy 2014). A previous report observed abnormal EMS divisions in *gpa-16(it143ts);goa-1(RNAi)* embryos imaged at the nonpermissive temperature from the end of the P1 division (Zhang *et al.* 2008). However, in these embryos, all ABa and ABp cells had abnormal cleavage plane orientations, and the P1 division was not analyzed, raising concerns about indirect effects.

Our analysis of *gpa-16(ts)* single mutants revealed that *(it143ts)* is a slow inactivating, variable, temperature-sensitive allele (see *Materials and Methods*). Further, when *gpa-16(it143ts);goa-1(RNAi)* embryos were upshifted at the one-cell or early two-cell stages, the P1 nucleus and spindle showed a complete failure to rotate onto the A/P axis in most embryos (Figure S2A), regardless of the timing of the upshift. Under these conditions, the EMS division was abnormal in 58% of *gpa-16(it143ts);goa-1(RNAi)* embryos (Figure S2A). However, in the subset of embryos where P2 division could be scored, the P2 and EMS cell cycles were usually synchronous (14/17), consistent with the failed rotation in the P1 cell. Thus, it is not clear whether P2 was correctly specified and competent to provide Wnt and Src signaling to the EMS. Additionally, all *gpa-16(ts)*; *goa-1(RNAi)* embryos had abnormal ABa/p divisions in which the cells often appeared to physically push into the EMS blastomere (Figure S2A). We were not able to separate EMS division defects from P1 and ABa/p abnormalities using partial knockdown conditions (see *Materials and Methods* for details). Changing the geometry of a cell can have an effect on its spindle orientation (Tsou *et al.* 2003b; Nestor-Bergmann *et al.* 2014). Thus, given our observations, it is not clear whether the EMS spindle defects exhibited by *gpa-16(ts)*; *goa-1(RNAi)* are a direct or indirect effect of loss of Gα activity.

Although GPA-16 and GOA-1 are partially redundant, loss of GPA-16 function alone results in failure of P1 rotation in 75% of embryos when *gpa-16(ts)* mutants are raised at 25° (Bergmann *et al.* 2003). Moreover, 31% EMS division defects in *gpa-16(ts)* embryos were previously described (Tsou *et al.* 2003a). However, again, P1 and AB divisions were not carefully followed and double-mutant analysis was not performed. Therefore, we upshifted *gpa-16(ts);GFP::tubulin* embryos before P1 division to at least partially inactivate the GPA-16(ts) protein and examined the EMS division. Although these conditions do not fully inactivate GPA-16 (see *Materials and Methods*), we reasoned that a partial loss-of-function could still enhance *wnt* or *mes-1* RNAi, if GPA-16 acts in one of these pathways. With this regimen, although the P1 spindle exhibited a failed or late rotation in some *gpa-16(ts)* embryos, in all embryos the ABa/p spindles

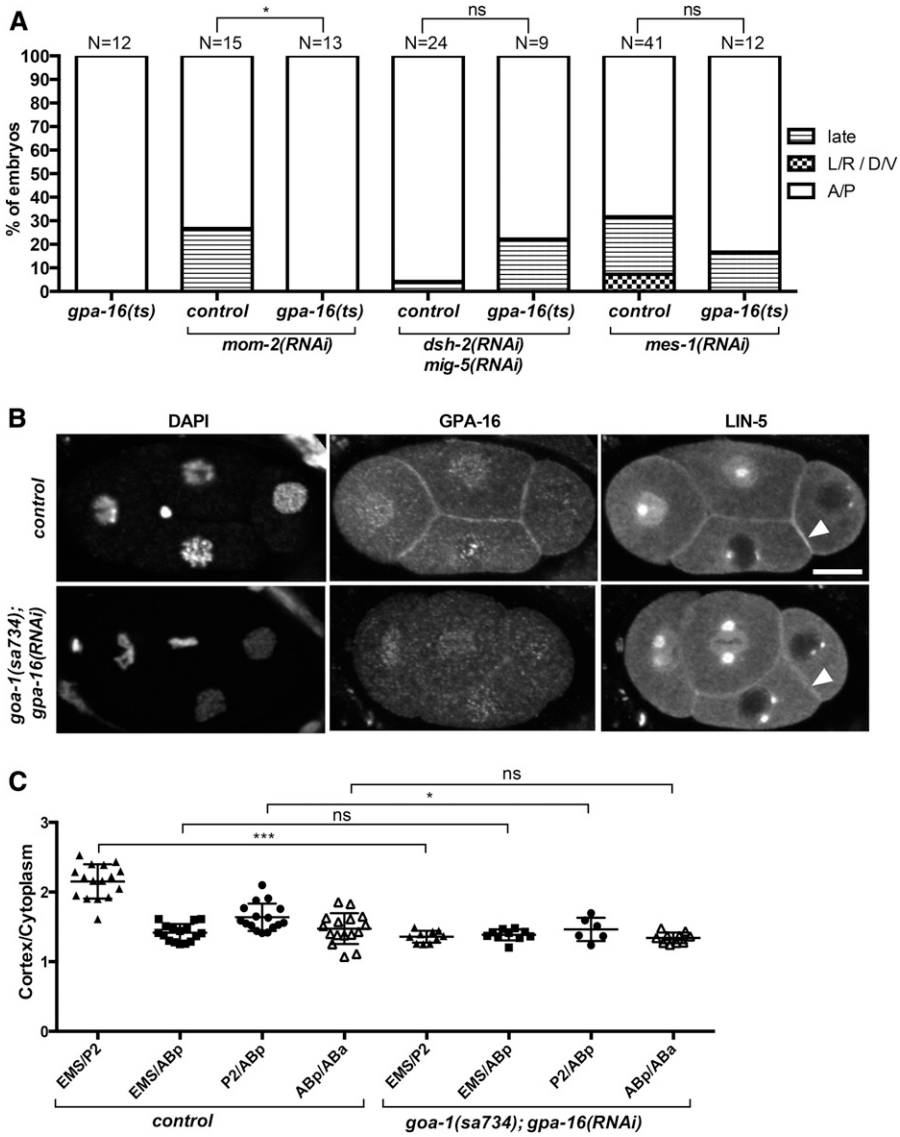

Figure 5 Cortical LIN-5 persists in Gα double-mutant embryos. (A) Quantification of spindle positioning in *gpa-16(it143ts)* embryos, alone or in combination with RNAi depletion of Wnt or Mes-1/Src-1 pathway components. The effectiveness of *mes-1(RNAi)* and *mom-2(RNAi)* treatments was confirmed by analyzing double *wnt*- and *mes-1*-mutant and RNAi combinations in parallel: 100% of *mes-1*; *mom-2(RNAi)* (N = 7), 92% of *mes-1*; *dsh-2:mig-2(RNAi)* (N = 12), and 100% of *mom-5*; *mes-1(RNAi)* (N = 5) embryos showed EMS spindle positioning defects. (B) Maximum fluorescence intensity Z projections of confocal images of LIN-5 and GPA-16 antibody staining in control and *goa-1(sa734)*; *gpa-16(RNAi)* embryos. Arrowheads mark the EMS/P2 cell contact sites. (C) Quantification of the maximum cortical intensity at the indicated cell–cell contact sites in control (N = 16) and *goa-1(sa734)*; *gpa-16(RNAi)* (N = 11) embryos; note that there are fewer P2/ABp contact sites in *goa-1(sa734)*; *gpa-16(RNAi)* embryos because abnormal AB and P1 divisions can result in embryos with four cells in a row. Data were compared using the unpaired Student's *t*-test (ns, not significant, $P > 0.05$, * $P \leq 0.05$, *** $P \leq 0.001$, see Table S2 for specific P values). A/P, anterior/posterior; D/V, dorso/ventral; EMS, endomesodermal precursor; L/R, left/right; NEB, nuclear envelope breakdown; RNAi, RNA interference.

set up correctly (Figure S2A). Those *gpa-16(ts)* embryos did not exhibit EMS spindle positioning defects, and *gpa-16(ts)* did not enhance either the *wnt* or *mes-1* single-mutant phenotypes (Figure 5A). These data suggest that GPA-16 alone is not required for EMS spindle positioning.

LIN-5 persists at the cortex in Gα double mutants

As an additional way to test if Gα may play a role in the EMS cell, we examined LIN-5 cortical localization. At the one-cell stage, cortical LIN-5 is barely detectable in Gα double RNAi embryos (Park and Rose 2008). Thus, we predicted that if GPA-16 and GOA-1 are the only anchors for LIN-5 cortical localization in EMS, cortical LIN-5 would be greatly reduced in Gα double mutants at the four-cell stage. Cortical LIN-5 staining intensities were measured at the cell contact sites of prophase to metaphase four-cell embryos in the same background used for the spindle positioning assay, *gpa-16(ts); goa-1(RNAi)*, as well as after *gpa-16* RNAi treatment of a predicted null allele of *goa-1*, *sa734* (Robatzek and Thomas 2000; Afshar *et al.* 2005). In control embryos, LIN-5 was present at higher levels at the P2/EMS cell–cell contact site compared to other EMS contacts, as previously reported (Figure 5B and Table S2) (Srinivasan *et al.* 2003; Fisk Green *et al.* 2004). LIN-5 enrichment at EMS/P2 was not present in Gα mutant embryos, and the levels at the ABp/P2 cell contact were also lower in Gα mutant embryos compared to wild-type. Nonetheless, there was still cortical accumulation at these contact sites and the levels at the EMS/ABp and ABp/ABa contacts were not significantly reduced (Figure 5, Figure S2B, and Table S2). The enrichment of GPR-1/2 to the P2/EMS cell contact was recently demonstrated to be in the P2 cell, rather than in the EMS cell (Werts *et al.* 2011). Thus, the loss of LIN-5 from the P2 contact sites in *Gα* double-mutant embryos is consistent with a model in which Gα anchors GPR-1/2 and LIN-5 to the cortex in the P2 blastomere. However, the persistence of LIN-5 at other cell contacts suggests that LIN-5 may be recruited to the cortex of early blastomeres, including EMS, in a Gα-independent manner.

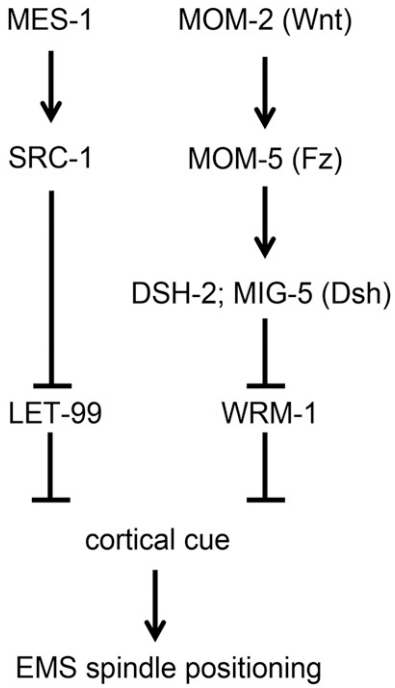

Figure 6 Model for the role of LET-99 signaling in EMS spindle positioning. Vertebrate orthologs of canonical Wnt pathway members are shown in parentheses. WRM-1 is a β-catenin-related protein.

Because we did not observe an obvious effect on LIN-5 cortical localization in Gα-depleted embryos, we considered other LIN-5 anchoring proteins for their potential role in EMS spindle positioning. In *Drosophila*, Dlg colocalizes with Pins, Mud, and Gα (Bellaiche *et al.* 2001b) and the *C. elegans* Discs Large protein, DLG-1, has been identified as a LIN-5 interacting protein in a yeast two-hybrid screen (Li *et al.* 2004). We hypothesized that DLG-1 may be involved in anchoring LIN-5 to the EMS cortex, and therefore its loss may result in defective spindle positioning. RNAi of DLG-1 resulted in 93% embryonic lethality as previously published (Maeda *et al.* 2001). However, we did not observe EMS spindle positioning defects in *dlg-1(RNAi)* embryos. In addition, there was no enhancement of Wnt or Mes-1/Src-1 pathway single-mutant phenotypes when combined with *dlg-1(RNAi)* (Figure S3A). Finally, the cortical localization of LIN-5 at the four-cell stage was not reduced in *dlg-1(RNAi)* embryos (Figure S3B).

Discussion

SRC-1 is an important player in EMS spindle positioning, but the molecular mechanism by which it affects nuclear rotation is unknown. This study provides evidence for the primary role of LET-99 in the Mes-1/Src-1 pathway and also reveals a role for LIN-5 in EMS spindle positioning.

LIN-5 interacts with regulators of the dynein microtubule motor and, thus, is likely to directly promote force generation for nuclear rotation in the EMS cell, as demonstrated in other cell types (Morin and Bellaiche 2011; McNally 2013). There are several models that are consistent with our data and a role for LIN-5 in EMS spindle positioning. First, LIN-5 may act downstream of both Wnt and Src-1 pathways. However, we predicted that if LIN-5 is in both pathways, *lin-5(ts)* would result in a complete failure of spindle alignment, as seen for *mes;wnt* double mutants, and this was not clearly observed. A second model, based on the precedent of LET-99 inhibiting GPR-1/2 and LIN-5 localization during the first asymmetric division (see below), is that LIN-5 acts only in the Mes-1/Src-1 pathway with LET-99. Interestingly, when the proportion of embryos with complete failure of spindle alignment (rather than combined late and failed rotations) is compared, *lin-5(ts);mom-2(RNAi)* embryos have significantly more defects than *lin-5(ts)* alone ($P = 0.022$), but *lin-5(ts); mes-1(RNAi)* do not ($P = 0.15$). Nonetheless, with this model, we would again predict a higher proportion of failed alignments. The lack of a strong phenotype in *lin-5(ts)* single- and double-mutant combinations could be due to failure to completely inactivate the available *lin-5(ts)* allele, if spindle positioning at the four-cell stage requires less force. Alternatively, LIN-5 may function redundantly with another force-generating machinery such as in *Drosophila* neuroblasts, where the LIN-5 ortholog, Mud, functions in parallel with a kinesin complex (Siegrist and Doe 2005; Johnston *et al.* 2009).

LET-99 has been studied in the context of intrinsic PAR polarity cues that regulate spindle positioning in the one-cell *C. elegans* embryo. LET-99 is asymmetrically localized at the cortex in a lateral band in the one-cell and in the P1 cell by the PAR polarity proteins. In this region, LET-99 inhibits the localization of GPR-1/2 and LIN-5 to the cortex, thus generating asymmetry of cortical pulling forces (Tsou *et al.* 2003a; Wu and Rose 2007; Park and Rose 2008; Krueger *et al.* 2010). At the four-cell stage, LET-99 is present in a band pattern in the P2 cell that divides asymmetrically in response to PAR cues. In contrast, the only asymmetry observed in the EMS cell is a lower level of LET-99 at the P2/EMS contact where GPR-1/2 and LIN-5 are enriched. Thus, it was previously proposed that LET-99 inhibits GPR-1/2 /LIN-5 recruitment to Gα at the cell cortex at all regions except the EMS/P2 cell contact, generating asymmetry of cortical GPR-1/2 /LIN-5 (Tsou *et al.* 2003a). In this scenario, Gα would function in the Mes-1/Src-1 pathway. However, based on the studies reported here, it is not clear whether Gα plays a direct role in EMS spindle positioning. We observed a correlation between failed EMS rotation and abnormalities of the ABa/p divisions (Figure S2A), and such ABa/p defects were observed in the previous studies that reported EMS spindle alignment defects in Gα mutants (Zhang *et al.* 2008). Further, we did not observe an enhancement of spindle positioning defects in *wnt; gpa-16(ts)* double mutants.

It is possible that GPA-16 and GOA-1's role in EMS is masked by redundancy with another Gα subunit. Alternatively, LET-99 and LIN-5 may act through a Gα-independent pathway in the EMS cell. Interestingly, our data show that cortical LIN-5 persists in Gα double mutants. This raises the possibility that LIN-5 is localized to the EMS cortex in a

Gα-independent manner. There have been multiple reports of LIN-5 orthologs recruited to the cortex by molecules other than Gαi. For instance, in *Drosophila* SOP cells and zebrafish epiblast cells during gastrulation, Dsh anchors NuMA to the cortex (Segalen *et al.* 2010). Moreover, the cortical localization of NuMA is LGN/ Gα-independent during anaphase of HeLa cells (Kiyomitsu and Cheeseman 2013; Kotak *et al.* 2014). NuMA has been shown to be capable of associating with phospholipids *in vitro* (Kotak *et al.* 2014; Zheng *et al.* 2014). In addition, the actin cytoskeleton has been shown to be required for cortical NuMA localization in keratinocytes and HeLa cells (Seldin *et al.* 2013; Kotak *et al.* 2014). Actin has also been implicated in zebrafish epiblast spindle positioning (Castanon *et al.* 2013) as well as in the division of ABar cell in the *C. elegans* early embryo, through a link to CED-10/Rac (Cabello *et al.* 2010). This poses an interesting possibility that the actin cytoskeleton may have a role in EMS spindle positioning.

The suppression of *mes-1* and *src-1* mutants by loss of *let-99* function suggests that LET-99 acts downstream of MES-1/ SRC-1 (Figure 6). Interestingly, the majority of the *let-99(ts); mes-1*; *mom-2(RNAi)* embryos display normal EMS spindle positioning at the nonpermissive temperature. This is reminiscent of the *wrm-1;mes-1;mom-2* triple-mutant phenotype. Although downregulation of WRM-1, a β-catenin-related protein, does not affect EMS spindle positioning, the spindle positioning phenotype of *mom-2;mes-1* double mutants is partially rescued in *mom-2;mes-1*;*wrm-1* triple mutants. WRM-1 is present all around the cortex of EMS at the beginning of the cell cycle, but is then asymmetrically localized to the anterior EMS cortex in response to the upstream Wnt pathway components. These results lead to the hypothesis that WRM-1 normally functions to mask an unidentified intrinsic polarity cue at the P2/EMS cell contact site that is capable of promoting proper EMS spindle positioning (Kim *et al.* 2013). Our genetic data support a model in which LET-99 acts analogously to WRM-1 (Figure 6); LET-99 may need to be inactivated by the Mes-1/Src-1 pathway to allow for EMS nuclear rotation. One tempting model is that the decreased LET-99 localization at the P2/EMS cell contact region compared to other cell contacts is a response to the Mes-1/Src-1 pathway (Tsou *et al.* 2003a). However, although recent quantitative analysis confirmed that the LET-99 signal is more uniform after *src(RNAi)* or *mes-1(RNAi)* treatments, this is not due to an increase at the P2/EMS cell contact but rather a decrease at other contacts (Werts *et al.* 2011). An alternative scenario is that SRC-1, which functions within the EMS cell, may inhibit the activity of LET-99 rather than its localization to achieve asymmetric cortical force generation. Overall, the current data are consistent with a model in which the role of the Wnt and Src pathways is to inactivate WRM-1 and LET-99, respectively, to unmask a cortical cue. The exact nature of this cortical cue and how it functions to promote EMS nuclear rotation remains to be determined.

In summary, our study identifies LET-99, a member of the DEPDC1 family of proteins, as a downstream component of the SRC-1 pathway. Although Src is a conserved tyrosine kinase functioning in cellular growth, proliferation, motility, and differentiation (Luttrell and Luttrell 2004), its role in spindle positioning is poorly understood. In addition to its role in the EMS division of *C. elegans*, Src has been implicated in spindle positioning in vertebrate cells. In HeLa cells, inhibition of c-Src resulted in mispositioned spindles and defects in centrosome-mediated aster formation (Nakayama *et al.* 2012). However, it is unclear whether the spindle positioning abnormalities were the result of short astral microtubules that could not reach the cortex or due to a direct role in regulating cortical forces. Our study raises the possibility that Src regulates cortical forces via a pathway involving LET-99 and LIN-5/ NuMA orthologs in vertebrate cells. Future work will determine the molecular mechanism by which LET-99 acts in the Src pathway in *C. elegans*, and whether other members of the DEPDC1 family play a role in spindle positioning.

Acknowledgments

We thank the Bowerman, McNally, Seydoux, and Wood laboratories for strains, and the Cram laboratory for the *src-1(RNAi)* clone. We thank Neil Willits, University of California (UC) Davis Department of Statistics, for assistance with the Chi-squared analysis. We also thank members of the Rose and McNally labs and the UC Davis SuperWorm group for helpful discussion, and N. Brown, D. Starr, B. Draper, and M. van Gompel for comments on the manuscript. Some strains were provided by the *Caenorhabditis* Genetics Center, which is funded by the National Institutes of Health (NIH) Office of Research Infrastructure Programs (P40-OD010440). This work was supported by the NIH (1R01-GM-68744) and by a National Institute of Food and Agriculture grant CA-D*-MCB-6239-H to L.R.

Literature Cited

Afshar, K., F. S. Willard, K. Colombo, D. P. Siderovski, and P. Gonczy, 2005 Cortical localization of the Galpha protein GPA-16 requires RIC-8 function during C. elegans asymmetric cell division. Development 132: 4449–4459.

Bei, Y., J. Hogan, L. A. Berkowitz, M. Soto, C. E. Rocheleau *et al.*, 2002 SRC-1 and Wnt signaling act together to specify endoderm and to control cleavage orientation in early C. elegans embryos. Dev. Cell 3: 113–125.

Bellaiche, Y., M. Gho, J. A. Kaltschmidt, A. H. Brand, and F. Schweisguth, 2001a Frizzled regulates localization of cell-fate determinants and mitotic spindle rotation during asymmetric cell division. Nat. Cell Biol. 3: 50–57.

Bellaiche, Y., A. Radovic, D. F. Woods, C. D. Hough, M. L. Parmentier *et al.*, 2001b The partner of inscuteable/discs-large complex is required to establish planar polarity during asymmetric cell division in Drosophila. Cell 106: 355–366.

Bergmann, D. C., M. Lee, B. Robertson, M. F. Tsou, L. S. Rose *et al.*, 2003 Embryonic handedness choice in C. elegans involves the Galpha protein GPA-16. Development 130: 5731–5740.

Berkowitz, L. A., and S. Strome, 2000 MES-1, a protein required for unequal divisions of the germline in early C. elegans embryos, resembles receptor tyrosine kinases and is localized to the

boundary between the germline and gut cells. Development 127: 4419–4431.
Brenner, S., 1974 The genetics of Caenorhabditis elegans. Genetics 77: 71–94.
Cabello, J., L. J. Neukomm, U. Gunesdogan, K. Burkart, S. J. Charette *et al.*, 2010 The Wnt pathway controls cell death engulfment, spindle orientation, and migration through CED-10/Rac. PLoS Biol. 8: e1000297.
Capowski, E. E., P. Martin, C. Garvin, and S. Strome, 1991 Identification of grandchildless loci whose products are required for normal germ-line development in the nematode Caenorhabditis elegans. Genetics 129: 1061–1072.
Castanon, I., L. Abrami, L. Holtzer, C. P. Heisenberg, F. G. van der Goot *et al.*, 2013 Anthrax toxin receptor 2a controls mitotic spindle positioning. Nat. Cell Biol. 15: 28–39.
Couwenbergs, C., J. C. Labbe, M. Goulding, T. Marty, B. Bowerman *et al.*, 2007 Heterotrimeric G protein signaling functions with dynein to promote spindle positioning in C. elegans. J. Cell Biol. 179: 15–22.
Cram, E. J., H. Shang, and J. E. Schwarzbauer, 2006 A systematic RNA interference screen reveals a cell migration gene network in C. elegans. J. Cell Sci. 119: 4811–4818.
David, N. B., C. A. Martin, M. Segalen, F. Rosenfeld, F. Schweisguth *et al.*, 2005 Drosophila Ric-8 regulates Galphai cortical localization to promote Galphai-dependent planar orientation of the mitotic spindle during asymmetric cell division. Nat. Cell Biol. 7: 1083–1090.
Du, Q., and I. G. Macara, 2004 Mammalian pins is a conformational switch that links NuMA to heterotrimeric G proteins. Cell 119: 503–516.
Encalada, S. E., P. R. Martin, J. B. Phillips, R. Lyczak, D. R. Hamill *et al.*, 2000 DNA replication defects delay cell division and disrupt cell polarity in early Caenorhabditis elegans embryos. Dev. Biol. 228: 225–238.
Fisk Green, R., M. Lorson, A. J. Walhout, M. Vidal, and S. van den Heuvel, 2004 Identification of critical domains and putative partners for the Caenorhabditis elegans spindle component LIN-5. Mol. Genet. Genomics 271: 532–544.
Goulding, M. B., J. C. Canman, E. N. Senning, A. H. Marcus, and B. Bowerman, 2007 Control of nuclear centration in the C. elegans zygote by receptor-independent Galpha signaling and myosin II. J. Cell Biol. 178: 1177–1191.
Hao, Y., Q. Du, X. Chen, Z. Zheng, J. L. Balsbaugh *et al.*, 2010 Par3 controls epithelial spindle orientation by aPKC-mediated phosphorylation of apical Pins. Curr. Biol. 20: 1809–1818.
Hyman, A. A., and J. G. White, 1987 Determination of cell division axes in the early embryogenesis of Caenorhabditis elegans. J. Cell Biol. 105: 2123–2135.
Johnston, C. A., K. Hirono, K. E. Prehoda, and C. Q. Doe, 2009 Identification of an Aurora-A/PinsLINKER/Dlg spindle orientation pathway using induced cell polarity in S2 cells. Cell 138: 1150–1163.
Kamath, R. S., A. G. Fraser, Y. Dong, G. Poulin, R. Durbin *et al.*, 2003 Systematic functional analysis of the Caenorhabditis elegans genome using RNAi. Nature 421: 231–237.
Kim, S., T. Ishidate, R. Sharma, M. C. Soto, D. Conte, Jr. *et al.*, 2013 Wnt and CDK-1 regulate cortical release of WRM-1/beta-catenin to control cell division orientation in early Caenorhabditis elegans embryos. Proc. Natl. Acad. Sci. USA 110: E918–E927.
Kiyomitsu, T., and I. M. Cheeseman, 2013 Cortical dynein and asymmetric membrane elongation coordinately position the spindle in anaphase. Cell 154: 391–402.
Kotak, S., C. Busso, and P. Gonczy, 2014 NuMA interacts with phosphoinositides and links the mitotic spindle with the plasma membrane. EMBO J. 33: 1815–1830.
Krueger, L. E., J. C. Wu, M. F. Tsou, and L. S. Rose, 2010 LET-99 inhibits lateral posterior pulling forces during asymmetric spindle elongation in C. elegans embryos. J. Cell Biol. 189: 481–495.
Li, S., C. M. Armstrong, N. Bertin, H. Ge, S. Milstein *et al.*, 2004 A map of the interactome network of the metazoan C. elegans. Science 303: 540–543.
Liu, J., L. L. Maduzia, M. Shirayama, and C. C. Mello, 2010 NMY-2 maintains cellular asymmetry and cell boundaries, and promotes a SRC-dependent asymmetric cell division. Dev. Biol. 339: 366–373.
Lorson, M. A., H. R. Horvitz, and S. van den Heuvel, 2000 LIN-5 is a novel component of the spindle apparatus required for chromosome segregation and cleavage plane specification in Caenorhabditis elegans. J. Cell Biol. 148: 73–86.
Luttrell, D. K., and L. M. Luttrell, 2004 Not so strange bedfellows: G-protein-coupled receptors and Src family kinases. Oncogene 23: 7969–7978.
Maeda, I., Y. Kohara, M. Yamamoto, and A. Sugimoto, 2001 Large-scale analysis of gene function in Caenorhabditis elegans by high-throughput RNAi. Curr. Biol. 11: 171–176.
McNally, F. J., 2013 Mechanisms of spindle positioning. J. Cell Biol. 200: 131–140.
Morin, X., and Y. Bellaiche, 2011 Mitotic spindle orientation in asymmetric and symmetric cell divisions during animal development. Dev. Cell 21: 102–119.
Nakayama, Y., Y. Matsui, Y. Takeda, M. Okamoto, K. Abe *et al.*, 2012 c-Src but not Fyn promotes proper spindle orientation in early prometaphase. J. Biol. Chem. 287: 24905–24915.
Nance, J., and J. R. Priess, 2002 Cell polarity and gastrulation in C. elegans. Development 129: 387–397.
Nestor-Bergmann, A., G. Goddard, and S. Woolner, 2014 Force and the spindle: mechanical cues in mitotic spindle orientation. Semin. Cell Dev. Biol. 34: 133–139.
Nguyen-Ngoc, T., K. Afshar, and P. Gonczy, 2007 Coupling of cortical dynein and G alpha proteins mediates spindle positioning in Caenorhabditis elegans. Nat. Cell Biol. 9: 1294–1302.
Park, D. H., and L. S. Rose, 2008 Dynamic localization of LIN-5 and GPR-1/2 to cortical force generation domains during spindle positioning. Dev. Biol. 315: 42–54.
Praitis, V., E. Casey, D. Collar, and J. Austin, 2001 Creation of low-copy integrated transgenic lines in Caenorhabditis elegans. Genetics 157: 1217–1226.
Robatzek, M., and J. H. Thomas, 2000 Calcium/calmodulin-dependent protein kinase II regulates Caenorhabditis elegans locomotion in concert with a G(o)/G(q) signaling network. Genetics 156: 1069–1082.
Rodriguez-Fraticelli, A. E., S. Vergarajauregui, D. J. Eastburn, A. Datta, M. A. Alonso *et al.*, 2010 The Cdc42 GEF intersectin 2 controls mitotic spindle orientation to form the lumen during epithelial morphogenesis. J. Cell Biol. 189: 725–738.
Rose, L., and P. Gonczy, 2014 Polarity establishment, asymmetric division and segregation of fate determinants in early C. elegans embryos. (December 30, 2014). *Wormbook*, ed. The *C. elegans* Research Community, WormBook, doi/10.1895/wormbook.1.30.2, http://www.wormbook.org.
Rose, L. S., and K. Kemphues, 1998 The let-99 gene is required for proper spindle orientation during cleavage of the C. elegans embryo. Development 125: 1337–1346.
Schlesinger, A., C. A. Shelton, J. N. Maloof, M. Meneghini, and B. Bowerman, 1999 Wnt pathway components orient a mitotic spindle in the early Caenorhabditis elegans embryo without requiring gene transcription in the responding cell. Genes Dev. 13: 2028–2038.
Segalen, M., C. A. Johnston, C. A. Martin, J. G. Dumortier, K. E. Prehoda *et al.*, 2010 The Fz-Dsh planar cell polarity pathway induces oriented cell division via Mud/NuMA in Drosophila and zebrafish. Dev. Cell 19: 740–752.
Seldin, L., N. D. Poulson, H. P. Foote, and T. Lechler, 2013 NuMA localization, stability, and function in spindle orientation involve 4.1 and Cdk1 interactions. Mol. Biol. Cell 24: 3651–3662.

Siegrist, S. E., and C. Q. Doe, 2005 Microtubule-induced Pins/Galphai cortical polarity in Drosophila neuroblasts. Cell 123: 1323–1335.

Siller, K. H., C. Cabernard, and C. Q. Doe, 2006 The NuMA-related mud protein binds pins and regulates spindle orientation in Drosophila neuroblasts. Nat. Cell Biol. 8: 594–600.

Srinivasan, D. G., R. M. Fisk, H. Xu, and S. van den Heuvel, 2003 A complex of LIN-5 and GPR proteins regulates G protein signaling and spindle function in C elegans. Genes Dev. 17: 1225–1239.

Strome, S., P. Martin, E. Schierenberg, and J. Paulsen, 1995 Transformation of the germ line into muscle in mes-1 mutant embryos of C. elegans. Development 121: 2961–2972.

Timmons, L., and A. Fire, 1998 Specific interference by ingested dsRNA. Nature 395: 854.

Tsou, M. F., A. Hayashi, L. R. DeBella, G. McGrath, and L. S. Rose, 2002 LET-99 determines spindle position and is asymmetrically enriched in response to PAR polarity cues in C. elegans embryos. Development 129: 4469–4481.

Tsou, M. F., A. Hayashi, and L. S. Rose, 2003a LET-99 opposes Galpha/GPR signaling to generate asymmetry for spindle positioning in response to PAR and MES-1/SRC-1 signaling. Development 130: 5717–5730.

Tsou, M. F., W. Ku, A. Hayashi, and L. S. Rose, 2003b PAR-dependent and geometry-dependent mechanisms of spindle positioning. J. Cell Biol. 160: 845–855.

Werts, A. D., M. Roh-Johnson, and B. Goldstein, 2011 Dynamic localization of C. elegans TPR-GoLoco proteins mediates mitotic spindle orientation by extrinsic signaling. Development 138: 4411–4422.

Williams, S. E., L. A. Ratliff, M. P. Postiglione, J. A. Knoblich, and E. Fuchs, 2014 Par3-mInsc and Galphai3 cooperate to promote oriented epidermal cell divisions through LGN. Nat. Cell Biol. 16: 758–769.

Wu, J. C., and L. S. Rose, 2007 PAR-3 and PAR-1 inhibit LET-99 localization to generate a cortical band important for spindle positioning in Caenorhabditis elegans embryos. Mol. Biol. Cell 18: 4470–4482.

Wu, J. C., E. B. Espiritu, and L. S. Rose, 2016 The 14–3-3 protein PAR-5 regulates the asymmetric localization of the LET-99 spindle positioning protein. Dev. Biol. 412: 288–297.

Zhang, H., A. R. Skop, and J. G. White, 2008 Src and Wnt signaling regulate dynactin accumulation to the P2-EMS cell border in C. elegans embryos. J. Cell Sci. 121: 155–161.

Zheng, Z., H. Zhu, Q. Wan, J. Liu, Z. Xiao *et al.*, 2010 LGN regulates mitotic spindle orientation during epithelial morphogenesis. J. Cell Biol. 189: 275–288.

Zheng, Z., Q. Wan, G. Meixiong, and Q. Du, 2014 Cell cycle-regulated membrane binding of NuMA contributes to efficient anaphase chromosome separation. Mol. Biol. Cell 25: 606–619.

Communicating editor: B. Goldstein

Figure S1. Spindle positioning in *let-99(or513ts)* embryos. (.ai, 382 KB)

www.genetics.org/lookup/suppl/doi:10.1534/genetics.116.192831/-/DC1/FigureS1.ai

Figure S2. Spindle positioning defects and LIN-5 cortical localization in Gα double mutants. (.ai, 750 KB)

www.genetics.org/lookup/suppl/doi:10.1534/genetics.116.192831/-/DC1/FigureS2.ai

Figure S3. EMS spindle positioning and LIN-5 localization in dlg-1(RNAi) embryos. (.ai, 440 KB)

www.genetics.org/lookup/suppl/doi:10.1534/genetics.116.192831/-/DC1/FigureS3.ai

Table S1. Statistical comparisons of spindle positioning abnormalities

Data analyzed	Genotypes compared	p-value
Centrosome migration		
Fig. 2B		
	control vs mes-1	0.54
	control vs mom-5	0.35
	control vs lin-5(ts)	0.44
	mom-5 vs mes-1	0.70
	control vs. mom-5; mes-1(RNAi)	0.93
	control vs let-99(ax218ts)	0.60
Spindle alignment		
Fig. 2C		
	mes-1 vs mes-1(RNAi)	0.092
	mes-1 vs mom-5	0.59
	mes-1 vs mes-1; mom-2(RNAi)	0.0049
	mom-5 vs mom-2(RNAi)	0.26
	mom-5 vs dsh-2(RNAi); mig-5(RNAi)	0.00099
	mom-5 vs mom-5; mes-1(RNAi)	0.00085
	control vs mom-5	0.00055
	control vs mes-1	0.00011
Fig. 3C		
	lin-5(ts) vs lin-5(ts); mom-2(RNAi)	0.11
	lin-5(ts) vs lin-5(ts); dsh-2(RNAi); mig-5(RNAi)	0.053
	lin-5(ts) vs lin-5(ts); mes-1(RNAi)	0.38
Fig. 4A		
	let-99(ts) vs let-99(ts); dsh-2(RNAi); mig-5(RNAi)	0.86
	mom-2(RNAi) vs let-99(ts); mom-2(RNAi)	0.67
	mes-1(RNAi) vs let-99(ts); mes-1(RNAi)	0.086
	src-1(RNAi) vs let-99(ts); src-1(RNAi)	0.018
Fig. 4B		
	mes-1 25°C vs let-99(ts); mes-1 25°C	0.022
	let-99(ts); mes-1; mom-2(RNAi)16°C vs let-99(ts); mes-1; mom-2(RNAi) 25°C	0.00057
	let-99(ts);mes-1; mom-2(RNAi) 16°C vs mes-1; mom-2(RNAi) 25°C	0.39
Fig. 5A		
	mom-2(RNAi) vs gpa-16(ts); mom-2 (RNAi)	0.044
	dsh-2(RNAi);mig-5(RNAi) vs gpa-16(ts);dsh-2(RNAi); mig-5(RNAi)	0.11
	mes-1(RNAi) vs gpa-16(ts); mes-1(RNAi)	0.31
Fig. S1		
	let-99(ts) vs let-99(ts);dsh-2(RNAi); mig-5(RNAi)	0.17
	mom-2(RNAi) vs let-99(ts); mom-2(RNAi)	0.088
	mes-1(RNAi) vs let-99(ts); mes-1(RNAi)	0.0637
	src-1(RNAi) vs let-99(ts); src-1(RNAi)	0.0022
Fig. S3		
	mes-1 vs mes-1; dlg-1(RNAi)	0.55
	mom-5 vs mom-5; dlg-1(RNAi)	0.48

Table S2. Comparison of LIN-5 and GPA-16 staining

	n	Relative cortical staining at specified contact sites (mean±sd) [a]				Comparison of contact sites in mutant to same contact site in control (p value) [b]			
		EMS/P2	EMS/ABp	P2/ABp	ABa/ABp	EMS/P2	EMS/ABp	P2/ABp	ABa/ABp
Anti-LIN-5 staining									
control	16	2.15±0.25	1.42±0.12[c]	1.64±0.20[c]	1.48±0.22[c]				
goa-1(sa734);gpa-16(RNAi)	11	1.35±0.09	1.36±0.10	1.43±0.18	1.33±0.08	1.5 e-10	0.25	0.026	0.051
gpa16(ts); goa-1(RNAi)	8	1.42±0.13	1.36±0.12	1.37±0.10	1.39±0.13	1.6 e-06	0.45	0.0019	0.78
dlg-1(RNAi)	9	1.97±0.19	1.33±0.09 [c]	1.51±0.14 [c]	1.45±0.20 [c]	0.068	0.07	0.11	0.78
Anti-GPA-16 staining									
control	8	1.75±0.18	1.48±0.26	1.58±0.27	1.74±0.61				
goa-1(sa734);gpa16RNAi	11	1.07±0.10	1.06±0.14	1.04±0.14	0.99±0.09	6.9 e-09	3. 2 e-04	3.5 e-04	7.4 e-04

[a] Mean cortical to cytoplasmic ratios of staining intensities, +/- standard deviation (sd).
[b] p values from unpaired Student's t-test for comparisons of the same contact site between genotypes, for the antibody staining indicated.
[c] Statistically significant ($p<0.05$) difference in LIN-5 cortical intensities, using unpaired Student's t-test for this cell contact compared to the EMS/P2 contact in the same genotype.